iScience

CellPress
OPEN ACCESS

Article

Ag/polydopamine-coated textile for enhanced liquid/liquid mixtures separation and dye removal

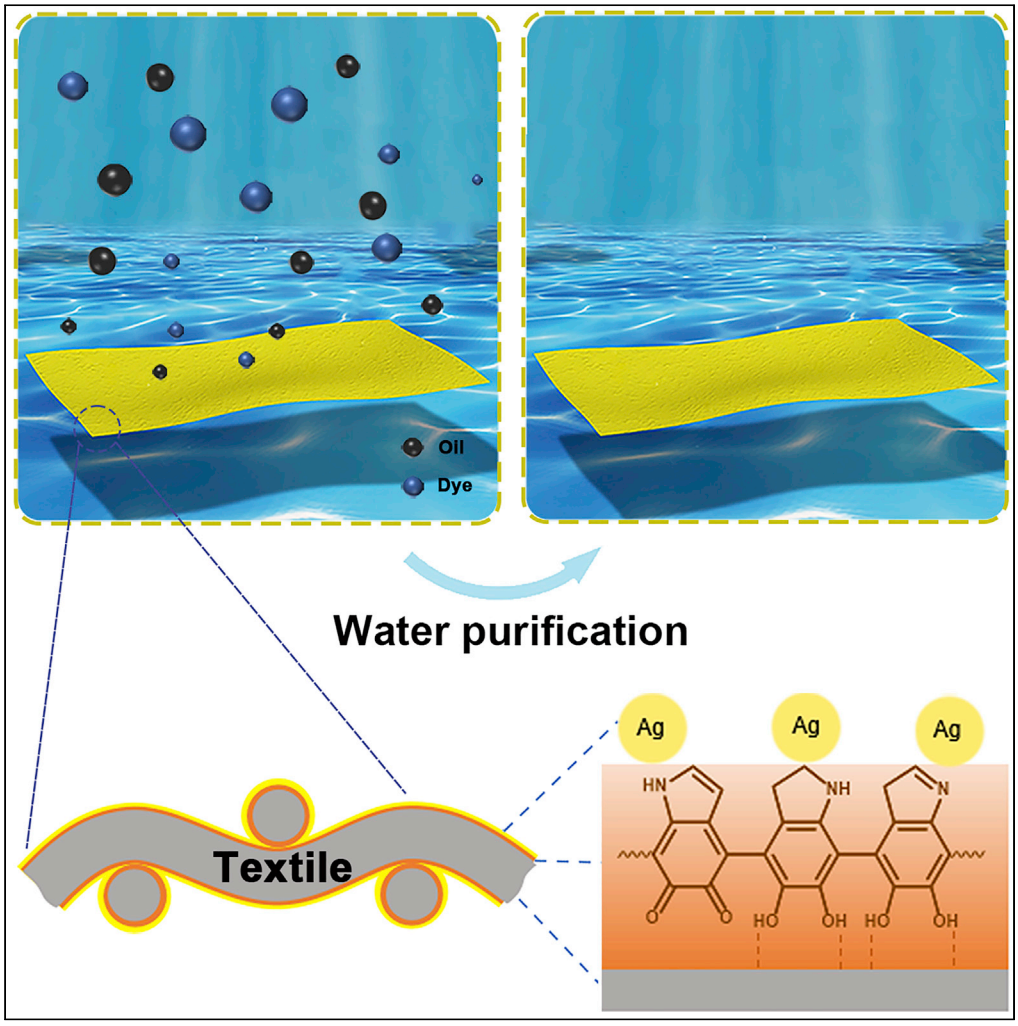

Gan Miao, Fangchao Li, Zhongshuai Gao, ..., Yuanming Song, Xiangming Li, Xiaotao Zhu

rgnlicp@126.com (G.R.)
xiaotao.zhu@ytu.edu.cn (X.Z.)

Highlights

A superhydrophilic/superoleophobic textile was fabricated

Both oil/water and oil/oil mixtures were separated successfully

Removing dye from water also achieved

Miao et al., iScience 25, 104213
May 20, 2022 © 2022 The Authors.
https://doi.org/10.1016/j.isci.2022.104213

iScience

CellPress
OPEN ACCESS

Article

Ag/polydopamine-coated textile for enhanced liquid/liquid mixtures separation and dye removal

Gan Miao,[1] Fangchao Li,[1] Zhongshuai Gao,[1] Ting Xu,[1] Xiao Miao,[2] Guina Ren,[1,*] Yuanming Song,[1] Xiangming Li,[1] and Xiaotao Zhu[1,3,*]

SUMMARY

Engineering a versatile platform that enables to separate both oil/water and oil/oil mixtures and remove dye from water is not easy. To address this challenge, we have developed an Ag/polydopamine-coated textile (Ag/PDA@textile) by chemically depositing Ag particles on the textile surface using polydopamine as the binder layer. The obtained Ag/PDA@textile attracts water but repels oil in the air, underwater, and when immersed into the oil. Exploiting its water-attracting and oil resistance, the Ag/PDA@textile is acted as a separation membrane to separate oil/water mixtures with enhanced separation efficiency. The Ag/PDA@textile also possesses opposite wetting behavior to oils with different polarities, allowing it to separate oil/oil mixtures efficiently. Thanks to the catalytic performance of the Ag particle, organic dyes can be decomposed effectively by our Ag/PDA@textile under UV illustration or in the presence of $NaBH_4$. Our Ag/PDA@textile may be valuable for applications in water purification and oil sewage treatment.

INTRODUCTION

The frequency of industrial oil-bearing wastewater, oil spills, and serious water pollution problems have increased rapidly in recent decades, seriously damaging human health and the ecological environment (Ge et al., 2016; Schrope, 2011; Wang et al., 2015a). Several methods, including flotation, gravity separation, flocculation, and oil-absorbing materials, have been traditionally applied to separate oil/water mixtures, while they are suffering limited selectivity, high energy consumption, low separation efficiency, and secondary pollution (Gupta et al., 2017; Yu et al., 2017). Designing porous surfaces that have the opposite wetting behavior of oil and water has been proven to be an effective way for the separation of oil/water, and this idea led to the production of numerous selective wettability membranes (Ma et al., 2016; Peng and Guo, 2016; Zhang et al., 2019). The superhydrophobic/superoleophilic surfaces (Wei et al., 2020; Yu et al., 2022), underwater superoleophobic surfaces, and superhydrophilic/superoleophobic surfaces are typically developed for separating different mixtures of oil/water (Qiu et al., 2020; Sarcletti et al., 2019; Zhang et al., 2018). Compared to superhydrophobic/superoleophilic surfaces and underwater superoleophobic surfaces, superhydrophilic/superoleophobic surfaces are much more suitable for oil/water separation, as they selectively filter water from oil and are more resistant to oil fouling, which is beneficial for durable separation efficiency and good recyclability (Dai et al., 2020; Lu et al., 2020; Tang et al., 2016; Yan et al., 2019; Zhang et al., 2014). However, engineering such a type of superhydrophilic/superoleophobic surface is hard to achieve, as the water surface tension is distinctly higher than the surface tension of most oils (Drelich and Chibowski, 2010; Jung and Bhushan, 2009; Wenzel, 1936; Xu et al., 2015). Recently, Yang et al. developed the air-plasma-triggered transition method to achieve both superhydrophilic and superoleophobic properties in one surface (Yang et al., 2012). Our group also manufactured a superhydrophilic/superoleophobic surface by blending a fluorinated segment and a polar hydrophilic segment (Lu et al., 2021). In practical applications, there are far more mixtures to be separated than just mixtures of oil/water, and separation of oil/oil mixtures is also an intractable problem (Mai et al., 2020; Tie et al., 2018; Wang et al., 2015b, 2017). Until now, oil/oil mixtures separation has rarely been studied, although oil/water separation has been extensively evaluated. The difficulty results from the truth that the surface tension difference between two oily liquids is far less than that between oil and water (Berg et al., 1994; Vogler, 1998). To meet the growing needs in the field of chemical industry, such as anhydrous heterogeneous chemical reactions, developing a selective wettability membrane that enables to separate both oil/water and oil/oil mixtures is highly desirable (Horváth and Rábai, 1994; Nyiredy et al., 1990).

[1]School of Environmental and Material Engineering, Yantai University, Yantai 264405, China

[2]Shandong Key Laboratory of Optical Communication Science and Technology, School of Physics Science and Information Technology, Liaocheng University, Liaocheng 252000, China

[3]Lead contact

*Correspondence: rgnlicp@126.com (G.R.), xiaotao.zhu@ytu.edu.cn (X.Z.)

https://doi.org/10.1016/j.isci.2022.104213

This is an open access article under the CC BY-NC-ND license (http://creativecommons.org/licenses/by-nc-nd/4.0/).

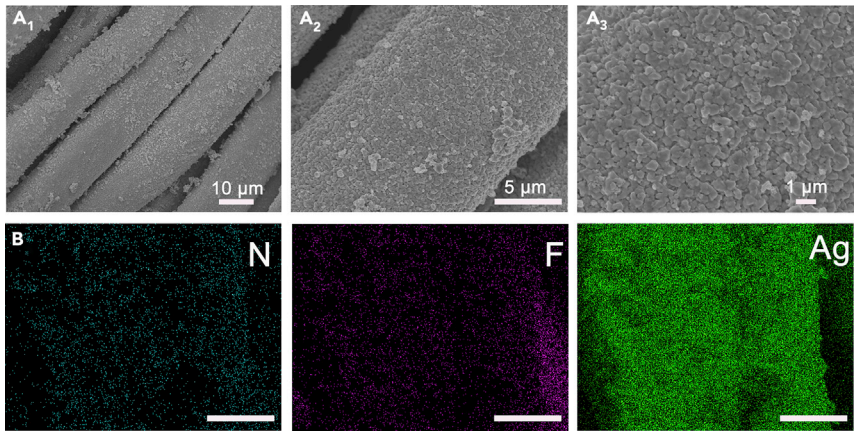

Figure 1. Surface topography and chemistry analysis of Ag/PDA@textile

(A and B) FESEM photographs of the obtained Ag/PDA@textile at low and high marginations (A1–A3); EDS mapping image of Ag/PDA@textile surface (B). The scales bar in image b is all 5 μm.

Besides oily wastewater treatment, dye pollution is also an urgent problem to be solved. Nowadays, over 280 thousand tons of dye wastewater are discharged into the environment annually, which leads to serious environmental pollution (Ai and Zeng, 2013; Tiwari et al., 2013). Owing to the varied chemical and physical characteristics of water-soluble dyes and water-insoluble oily liquids, one method usually only works for one of the two contaminants. Therefore, there is an urgent demand for a multifunctional platform that can achieve oily wastewater treatment and dye wastewater purification. In this study, we have developed an Ag/PDA@textile by chemically depositing Ag particles on the textile surface using polydopamine as the binder layer, and it is capable to separate both oil/water and oil/oil mixtures and remove dyes from water. The obtained Ag/PDA@textile exhibited both water-affinity and oil-repellency in air, displayed superoleophobicity underwater, and resisted oil fouling when immersed into the oil. Utilizing this opposite wettability for oil and water, the Ag/PDA@textile could act as a separation membrane to filter water from oil selectively, and its slippery oil repellency prevents it from being contaminated by oil. The Ag/PDA@textile also displays high repellency to low-polar oils but exhibits a great affinity for highly polar oils, enabling it to separate immiscible oil/oil mixtures with different polarities efficiently. Owing to the catalytic performance of the Ag particle (Zheng and Wang, 2012), organic dyes dissolved in water are decomposed effectively by the Ag/PDA@textile under UV illustration, and the dye decomposition can be accelerated significantly with the help of $NaBH_4$. This work would offer an effective method for liquid/liquid mixtures separation, wastewater treatment, and water purification.

RESULTS AND DISCUSSIONS

Surface topography and chemistry analysis

Figure 1 shows the SEM images and elemental distribution maps of the Ag/PDA@textile surface. The resulting sample surface is not smooth, and each micro-scale fiber is evenly covered with an Ag layer, as shown in Figure 1A. High-magnification images show that the Ag layer consists of Ag particles in the range of 70–230 nm. EDS analysis shows that the nitrogen (N) and silver (Ag) elements are well distributed on the textile surface (Figure 1B), indicating the successful PDA and Ag deposition; among them, the silver content is as high as 63.01% (Figure S1), means potential conductivity (Figure S2). After the pristine textile was modified by PDA, new peaks appeared at 1597 cm^{-1}, 1512 cm^{-1}, and 1152 cm^{-1} which are ascribed to C=C stretching vibration, N-H scissoring vibration, and the C-O stretching vibrations, respectively, as shown in Figure S3A. The band located at 1341 cm^{-1} is ascribed to the phenolic O-H stretching vibration in PDA, suggesting that PDA has successfully adhered on textile through the self-polymerization of DA (Chen et al., 2021). Furthermore, compared with the spectrum of PDA@textile, the characteristic peaks at 1341 cm^{-1} and 1152 cm^{-1} in Ag/PDA@textile were decreased significantly, indicating that redox reactions reaction between PDA and Ag^+ successfully consumed the O-H bond (Niyonshuti et al., 2020).

XPS analysis was also developed to study the reaction process between Ag^+ and PDA. As shown in Figure S3B, the surface of the pristine textile exhibits C 1s and O 1s peaks, but Ag/PDA@textile surface shows two new peaks, namely, N 1s Ag 3days, which are consistent with the EDS analysis results. Figure S3C

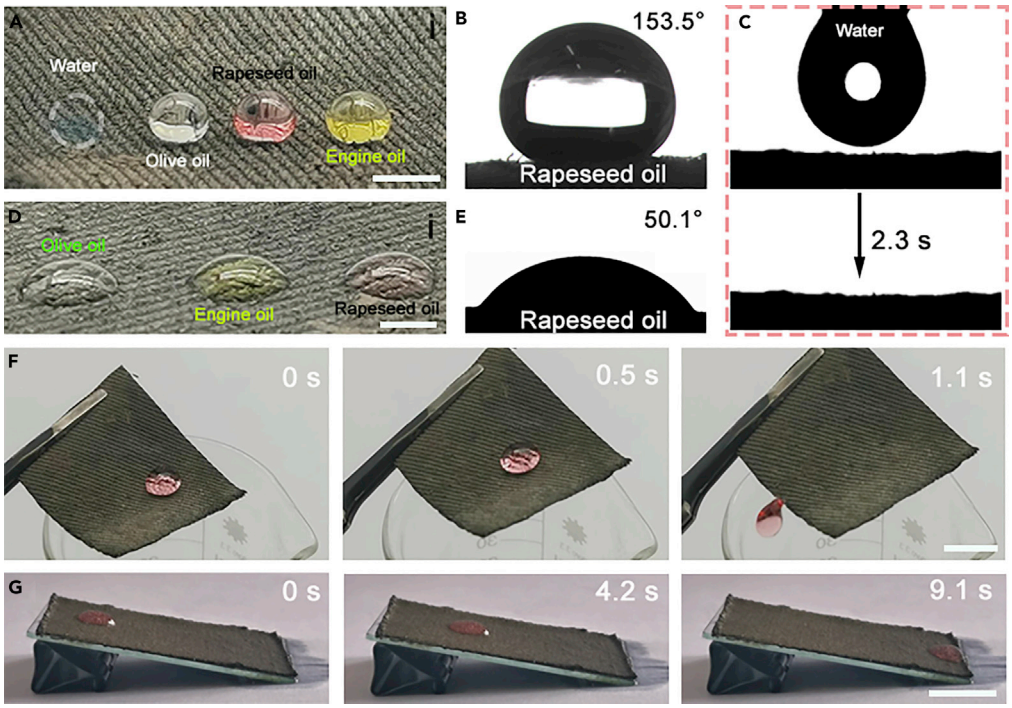

Figure 2. Wetting behavior analysis of Ag/PDA@textile in the air surrounding

(A–G) Water and oil droplets on the dry (A) and water-wetted (d) Ag/PDA@textile surface after coating with PFOA-Na; Water droplet can wet the resulting surface completely within 2.3 s (C); Contact angle profiles of rapeseed oil on the dry (B) and water-wetted (E) surface; The rapeseed oil was moving freely on the textile surface before (F) and after (G) being wetted by water. The scale bar of images a and d is 3 mm, and the scale bar of images f and g is 1 cm.

presents the high-resolution C 1s spectrum of the pristine textile, which can be deconvoluted into three peaks designated as the C-C/C-H bond at 284.52 eV, the C-N/C-O bond at 286.24 eV, and the C=O bond at 287.42 eV, respectively. As shown in Figure S3D, the binding energies of the C-C/C-H bond, C-N/C-O bond, and C=O bond in the high-resolution C 1s spectra of the Ag/PDA@textile are 284.54, 286.42, and 288.12 eV, respectively. The increase in the ratio of C-N and C-O is ascribed to the -NH-, R-NH_2 in PDA. In addition, in the Ag 3days spectrum of the Ag/PDA@textile, the peaks for Ag 3days positioned at 368 eV and 374 indicate that Ag^+ is successfully reduced (Zhu et al., 2012). The phenomenon is caused by the interaction between Ag^+ and catechol in PDA (Chen et al., 2021). The fluorine (F) element is also detected on the resulting Ag/PDA@textile surface, and its content is as low as 2.35% (Figure S1). This decrease in the use of fluorocarbons contributes to environmental protection and cost reduction (McFarland, 1992).

Wetting behavior in the air surrounding

The Ag/PDA@textile had both superoleophobic and superhydrophilic properties in the air environment, after coating with PFOA-Na. Oil droplets such as olive oil, rapeseed oil, and engine oil still showed spherical shape on the resulting textile surface with CA values all bigger than 150° and SA values all less than 9°, as shown in Figure 2A. For example, rapeseed oil with a contact angle of 153.5° (see Figure 2B) could roll down textiles easily with a slight tilt, as shown in Figure 2F. This superoleophobic fabric also possessed superhydrophilicity in air. Figure 2C showed that a water droplet was able to wet the fabric surface immediately and completely (less than 2.3 s).

This superhydrophilic/superoleophobic fabric also displayed oil-repellent properties after being wetted by water. As shown in Figure 2D, the oil contact angle profile was changed significantly, and oil droplets seemed to be floating on the water-wetted fabric surface with a contact angle of 50.1° (as shown in Figure 2E). Owing to its extremely strong water affinity, the layer of water around the fabric surface could function as a lubricant to repel oil (Yong et al., 2017). As shown in Figure 2G, rapeseed oil was moving freely on the water-wet fabric surface, with the help of the fluidity of the water lubricant.

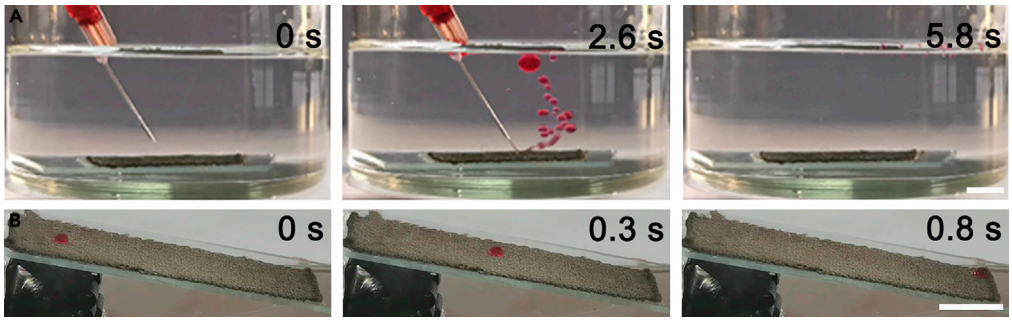

Figure 3. Wetting behavior analysis of Ag/PDA@textile in the water surrounding

(A and B) The oil-jetting test (A); The chloroform droplet was moving freely on the Ag/PDA@textile surface underwater (B). For easy observation, the toluene and chloroform were all dyed with oil red. The scale bar is 1 cm.

The solid surface total surface energy was comprised of the polar surface energy component (γp s) and the dispersive surface energy component (γd s), which can be treated independently (Fowkes, 1964; Owens and Wendt, 1969; Rabinovich and Derjaguin, 1988). For our Ag/PDA@textile, the fluorinated groups could reduce the γd s composition, resulting in high oil repellency. On the contrary, the hydrophilic COO^- and Na^+ increase the γp s component, leading to a strong water affinity. The water-affinity and oil-repellency of the coating are enhanced when the silver particles increase the surface roughness (see Methods S1 for details). Consequently, the resulting Ag/PDA@textile shows both superhydrophilic and superoleophobic properties.

Wetting behavior in the water surrounding

The obtained Ag/PDA@textile exhibited underwater superoleophobicity for all probing oil droplets, with oil contact angle values all greater than 150° and sliding angle values smaller than 9°. Figure 3A shows that a jet of toluene can bounce off the surface easily underwater without leaving any trace, which implied that the oil adhesion force adhesion on the surface was weak. Also, the chloroform droplet was moving freely on Ag/PDA@textile surface inclined slightly, and it took only 0.8 s to reach the surface end, further demonstrating the excellent underwater oil repellency of the Ag/PDA@textile, as shown in Figure 3B. When immersed into water, a hydrated layer was formed around the textile surface, which was able to decrease the solid-oil interface area and weaken the oil adhesiveness on the surface, resulting in superoleophobic property underwater (Matsubayashi et al., 2017).

Wetting behavior in oil surrounding

The surface wettability of the Ag/PDA@textile under oil was also studied. Interestingly, the mirror phenomenon was observed on the Ag/PDA@textile surface wetted by water when immersed in an oil bath (as shown in Figure 4A). This is because the water layer around the Ag/PDA@textile surface could serve as a shield to avoid the oil from penetrating the surface (Larmour et al., 2007). After one day of complete immersion in oil, the water layer was still stable and could repel oil, which enabled the Ag/PDA@textile surface to be completely clean without any oil penetration when taken out (as shown in Figure 4B). To further study the strength of this hydrated layer, we tested the contact angle of water in an oil environment (noted as WCA-O). Figure 4C showed that water droplet could spread on its surface completely within 0.9 s and displayed a WCA-O of 0° eventually when contacting the Ag/PDA@textile immersed into the oil. The above results indicated that the Ag/PDA@textile possessed a higher affinity for water than oily liquids even after immersion in oil bath, allowing the surface-bound water layer difficulty to be replaced by oil, and thus it exhibited anti-oil-fouling properties in oil surrounding.

Stability of the Ag/PDA@textile surface

The robustness of the non-wettable surface and durability are crucial for their practical application (Guan et al., 2020; Han and Gong, 2021; Liu et al., 2017; Zhang et al., 2021). Herein, our created Ag/PDA@textile surface maintained its oil repellency after more than 30 days of exposure to air, indicating its good long-term stability. It also possessed mechanical stability. As shown in Figures 5A and 5B, the Ag/PDA@textile still displayed oil-repellent property after tape-peeling and hand-twisting tests, and oil droplets such as hexadecane and rapeseed oil were moving freely on the tested surface. A linear abrasion test was then

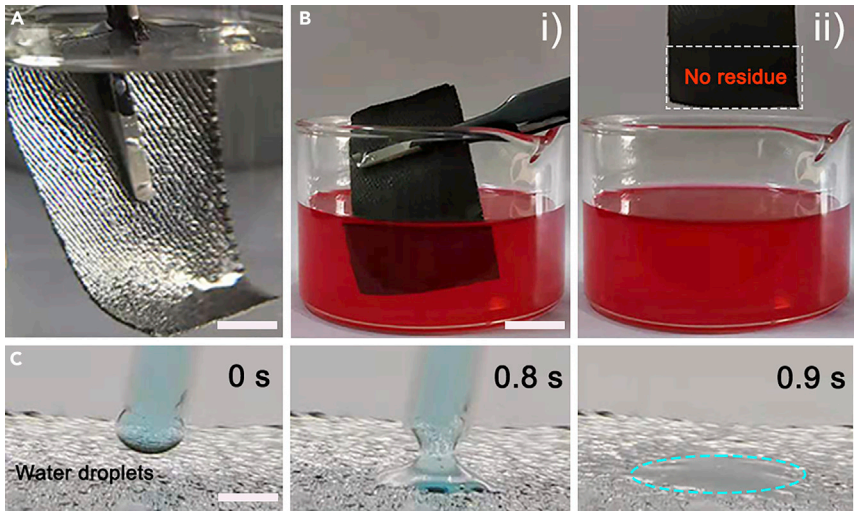

Figure 4. Wetting behavior analysis of Ag/PDA@textile in the oil surrounding

(A–C) The mirror phenomenon was observed on the Ag/PDA@textile surface wetted by water when immersed in oil (A); No dyed oil was left on the water-wetted Ag/PDA@textile surface even after 1 day of complete immersion in oil (B); Water droplets (colored with MB) can completely wet the surface of Ag/PDA@textile immersed in oil in less than 1 s (C). The scale bar is 50 mm.

conducted to fully investigate the mechanical robustness of the obtained Ag/PDA@textile. Sandpaper was used as the abradant. The Ag/PDA@textile weighting 100 g was tested to face the sandpaper and then moved back and forth with the abrasion length of 9 cm (see Figure 5C). The result showed that the rough surface texture was kept, and oil droplets showed spherical shape on the Ag/PDA@textile even after 10 cycles of abrasion test, as shown in Figure 6. Importantly, the Ag/PDA@textile still displayed superoleophobic to rapeseed oil (with CA more than 140°) even after 30 cycles of abrasion test, as shown in Figure S4. Owing to its inherent flexibility, the surface roughness of the Ag/PDA@textile was efficiently protected, when facing mechanical contact and distortion. In addition, the strong adhesion property of PDA molecular allows the Ag to bond the textile firmly, further improving the mechanical robustness of the Ag/PDA@textile. Moreover, the Ag/PDA@textile was also tolerant to long-term water immersion. Both the rapeseed oil contact angle and sliding angle were almost unchanged even after 24 h of full water immersion (see Figure 5D), and the water-wetted Ag/PDA@textile still showed the slippery oil-repellent properties.

Oil/water separation

The resulting Ag/PDA@textile had both water-affinity and oil-repellency, which allowed it to be a good choice for oil/water separation. As shown in Figure 7A, when the toluene/water mixture was poured on the Ag/PDA@textile, the water penetrated the textile and flowed down to the beaker below, but the

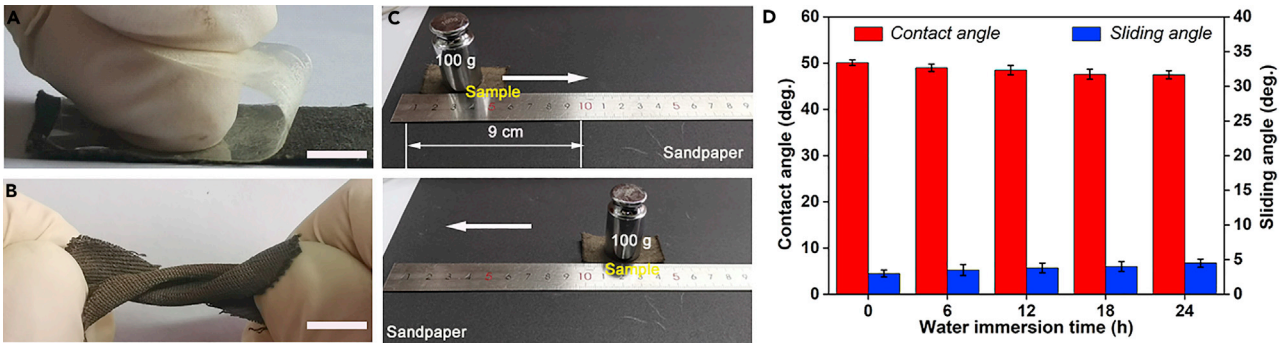

Figure 5. Stability of the Ag/PDA@textile surface

(A–D) Oil repellency is maintained after tape peeling (A), curling (B), and sandpaper sanding (C) of Ag/PDA@textile; Change of CAs and SAs of oil with water immersion time (D). Both contact and sliding angle were measured five times; the scale bar is 1 cm.

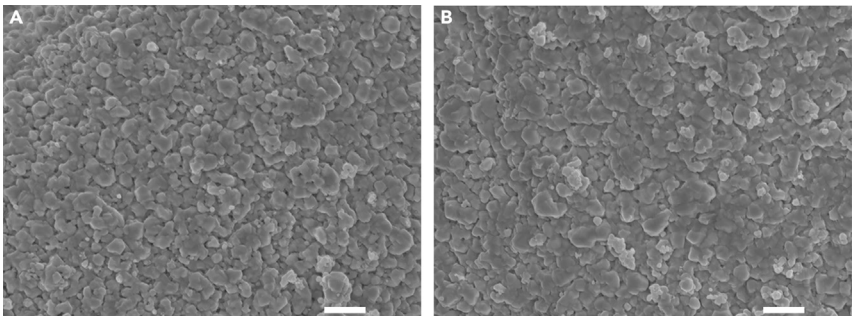

Figure 6. Surface topography analysis of Ag/PDA@textile after sandpaper sanding

(A and B) FESEM images of the obtained Ag/PDA@textile before (A) and after (B) sandpaper sanding. The scale bar is 1 μm.

toluene droplets (dyed oil red) remained on the surface of the textile without any penetration. The water separation rate (namely permeating flux) for the separation membrane was 1502 L m^{-2} h^{-1} bar^{-1} and it was changing slightly after 10 cycles of oil-water separation (see Figure S5). Interestingly, the Ag/PDA@textile can also be applied for separating oil/hot water separation. As shown in Figures 7B and 7C, when the toluene/hot water (80.5°) mixture was poured onto the textile, hot water passed through the textile quickly, but the toluene phase was kept in the top glass tube. The separation efficiency for the toluene/hot water mixture was still as high as 99%. This successful separation of hot water/oil mixture is of great significance to expand the application fields of our separation membrane and also to improve its durability under harsh environments (Yan et al., 2015). Thanks to its enhanced oil repellency, residual oil on the textile surface can be completely removed by simply rinsing with water after oil-water separation. As shown in Figure 7D, this anti-oil-fouling property of the Ag/PDA@textile enabled it to retain its improved separation efficiency even after ten cycles of oil/water separation. Besides, even surfactant-stabilized oil-in-water emulsions can be separated in the same way (as shown in Figure S6).

Oil/oil separation

Compared to the separation of oil/water, oil/oil separation was much more difficult to realize and had been rarely studied (see Table S1), because the surface tension difference between two oily liquids is far less than that between oil and water (Berg et al., 1994). Herein, the Ag/PDA@textile displayed opposite wetting behavior between the oily liquids with low and high polarity (see Figure 8A). This special wetting property enabled our Ag/PDA@textile to be ideal for oil/oil separation. When the ethylene glycol/rapeseed oil mixture (denoted as EG/RO) contacted the Ag/PDA@textile surface, as shown in Figure 8B, the highly polar EG permeates the textile and then collects in the beaker below, while the low polar RO remains above the

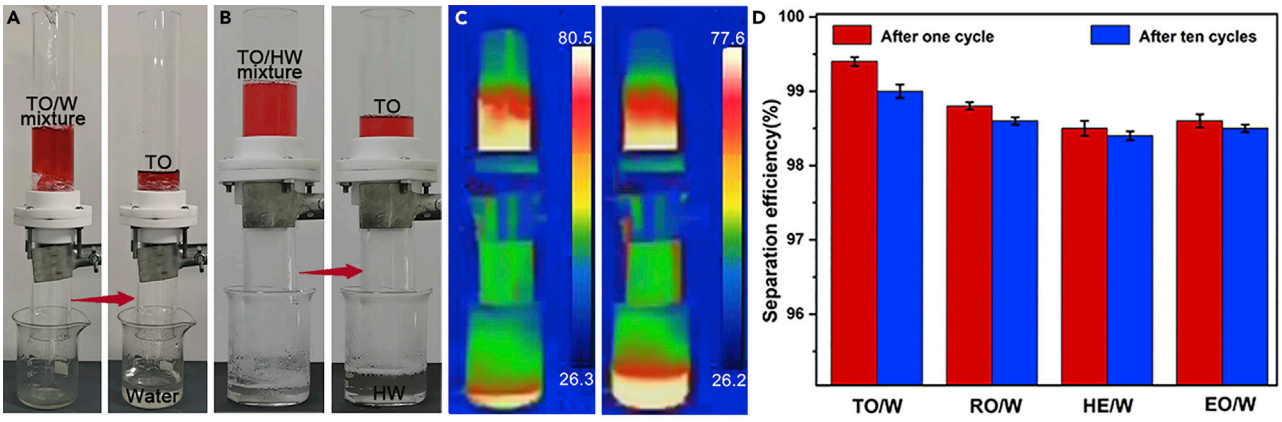

Figure 7. Oil/water separation capability of Ag/PDA@textile

(A–D) Ag/PDA@textile was used as separation membranes for separation of oil/water mixture (A); Optical (B) and infrared thermal (C) image of hot water/oil separation; A slight change in separation efficiency after 10 oil/water separation cycles (D). TO, RO, HE, and EO in Figure 7 represent toluene, rapeseed oil, hexadecane, and engine oil, respectively. The separation efficiency of each oil-water mixture was calculated five times.

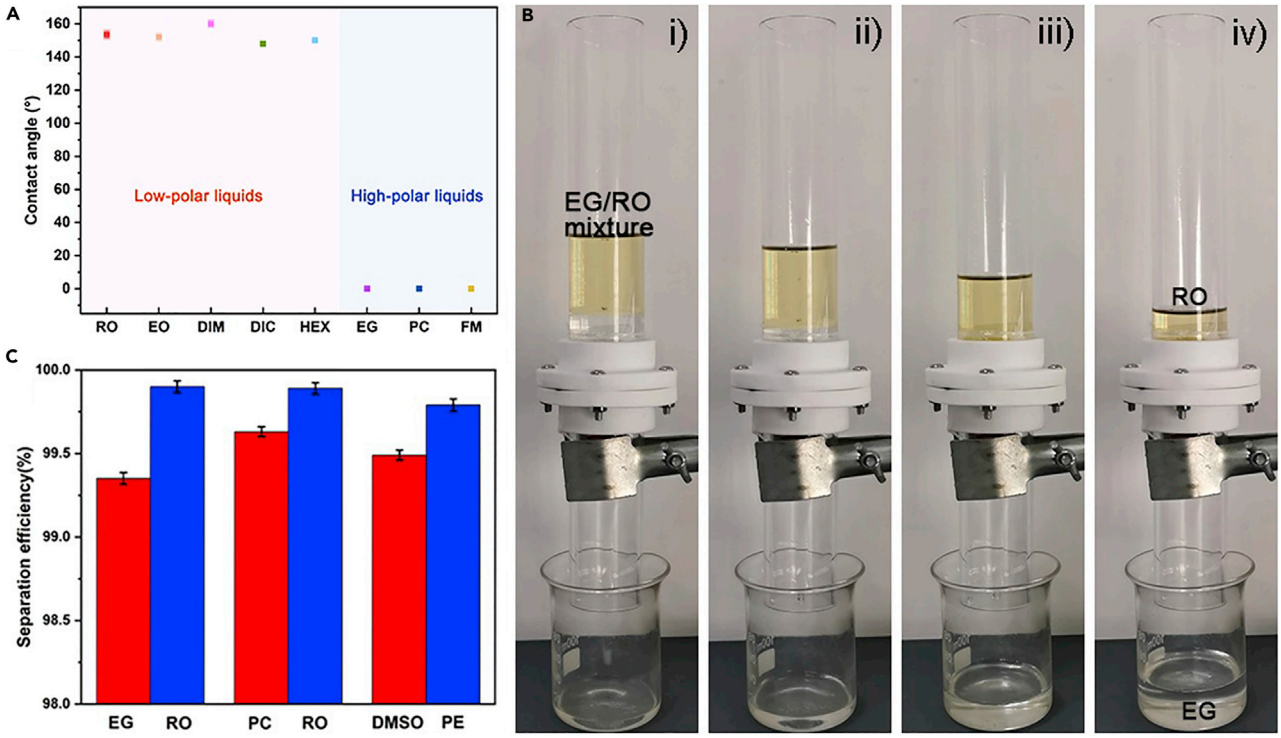

Figure 8. Oil/oil separation capability of Ag/PDA@textile

(A–C) CAs of the different probing oils (A); Ag/PDA@textile was used as separation membranes for oil/oil separation (B); Oil/oil separation efficiency of separation membranes (C). EO, EG, PC, DMSO, DIM, PE, DIC, and FM in Figure 8 represent engine oil, ethylene glycol, propylene carbonate, dimethyl sulfoxide, diiodomethane, petroleum ether, dichloroethane, and formamide, respectively. The separation efficiency of each oil/oil mixture was calculated five times.

textile surface because it presents an affinity for EG and repellency for RO. There was no visible RO in the filtered EG phase and the separation efficiency exceeded 99%; even under vigorous mechanical stirring, the EG/RO mixture can be separated in the same way (Figure S7), indicating successful oil/oil separation.

Based on recent studies, the surface can possess a high-polar-liquids affinity but a low-polarity-liquids repulsion provided that it has both the large enough γp s and sufficiently little γd S (Fowkes, 1964; Fowkes et al., 1988; Ge et al., 2016). For our Ag/PDA@textile, the fluorinated component minimized the γd S component, and the hydrophilic group improved the γp s component (see Methods S1 for details). Therefore, γp s was much larger than γd S, and when the Ag/PDA@textile surface was in contact with the probe liquid, the polar interaction dominated. Therefore, the Ag/PDA@textile exhibited oleophilic to highly polar liquids but displayed oleophobic to low polarity liquids. Taking advantage of Ag/PDA@textile opposite wetting to oils with different polarities, the Ag/PDA@textile can be used for separate immiscible mixtures of oil/oil with varied polarities, as shown in Figure 8C.

Organic dye removal performance

The emission of dye wastewater leads to severe environmental pollution (Qamar et al., 2021). Herein, the Ag/PDA@textile could act as an advanced platform for removing dye from water, due to the photocatalytic performance of the Ag particle (Chen et al., 2010). We choose MB as a tested organic pollutant to explore the photocatalytic performance of our Ag/PDA@textile. The Ag/PDA@textile was placed in MB aqueous solution under UV irradiation at room temperature. The color of MB aqueous solution was varying from blue to clear with the increase of UV irradiation time. UV-vis spectrum analysis demonstrated that the content of MB was decreasing gradually as the duration of UV exposure increased, and the MB aqueous solution became clean after 8 h of UV irradiation, as shown in Figure 9A and its inset. Moreover, the analysis of the removal limits for Ag/PDA@textile has shown that the Ag/PDA@textile could be recycled and reused at least 20 times with a stable catalytic removal of MB (as shown in Figure S8). With the help of $NaBH_4$, the MB decomposition by our Ag/PDA@textile can be accelerated significantly. The concentration of MB in the

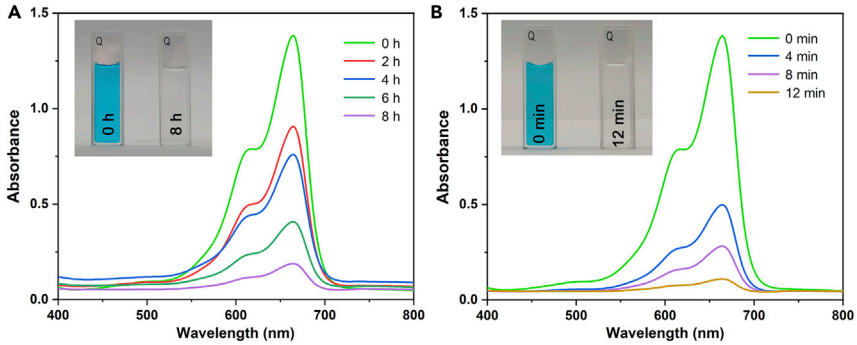

Figure 9. The organic dye removal performance of Ag/PDA@textile

(A and B) The color variation and UV-vis spectrum of MB aqueous solution as a function of UV irradiation time (A) and $NaBH_4$ reaction time (B).

water significantly decreases only after 12 min of reaction, leaving clear water eventually, as shown in Figure 9B. However, the absorbance intensity of MB in water was decreasing slightly even after 30 min reaction with $NaBH_4$, provided that the Ag/PDA@textile was not added into the MB aqueous solution, implying the important role of Ag/PDA@textile in the acceleration of MB decomposition.

This accelerated MB decomposition was attributed to the quick electron transfer progress caused by the synergistic effect between the Ag particles and $NaBH_4$ (Xie et al., 2014). Silver nanoparticles were good photocatalysts under ambient temperature for degrading organic compounds (Chen et al., 2010; Sarina et al., 2013). The photocatalytic activities of silver nanoparticles were attributed to the localized surface plasmon resonance (SPR) effect (Garcia, 2011). As reported by Chen and co-workers (Chen et al., 2010), UV could induce photocurrent on silver nanoparticles; i.e., the UV light could be absorbed by silver nanoparticles, exciting the conduction electrons through the SPR effect. These electrons with high energy could be captured by oxygen molecules on the surface of silver nanoparticles, resulting in the formation of strong oxidizing agents such as free radicals of hydroxyl (OH·) and super-oxygen ions (O− 2); meantime, the positive charges (holes) and/or silver ions would be created on the silver nanoparticles (Akram Shaikh et al., 2018). Free radicals of OH· and super-oxygen ions (O− 2) could readily oxidize MB into small molecules of H_2O and CO_2 (Kang et al., 2000; Karthik et al., 2017; Khare et al., 2018; Sahoo et al., 2005; Singh and Mehata, 2019; Wu et al., 2010).

The reduction mechanism of MB by $NaBH_4$ in the presence of Ag/PDA@textile can be explained by electron transfer progress. Briefly, the catalytic reduction follows an electrochemical mechanism where the silver nanoparticles act as redox catalysts through electron relay between MB and BH-4 (Islam et al., 2020; Sharif et al., 2019). Because of the high surface area of Ag/PDA@textile and the presence of the amino-functional group, BH-4 and MB are first adsorbed on the surface of Ag/PDA@textile. The nucleophilic BH-4 ions with high electron ejection capacity cathodically polarize the silver nanoparticles on the Ag/PDA@textile and then the electrophilic dye captures electrons from the electron-rich Ag nanoparticles and is reduced (the process are shown as following).

$nNaBH_4 \rightarrow nBH\text{-}4 + ne^- + Ag/PDA@textile \rightarrow e^- + MB \rightarrow Reduction$ (Islam et al., 2020; Sharif et al., 2019) It should be noted that the removal of dyes by our Ag/PDA@textile was not limited to MB, and other dyes dissolved in water such as Congo red were also able to be removed under UV irradiation or in the presence of $NaBH_4$.

Antibacterial property

The practical use of textiles under humid environments requires them to possess antibacterial properties (Lee et al., 2018; Xu et al., 2017). Herein, our resulting Ag/PDA@textile displayed antibacterial property, due to the inherent property of Ag particles (Wang et al., 2014). The antibacterial performance of our Ag/PDA@textile was evaluated by testing it against common bacteria, *Escherichia coli* (Gram-negative). The *E. coli* was incubated on the agar plates in the presence of Ag/PDA@textile, and then the growth status of the colony was analyzed by measuring the density of the colony. As shown in Figure 10A, no colony was found on the agar plate containing Ag/PDA@textile after incubation for 7 days. While the *E. coli* without Ag/PDA@textile was growing well on the agar plate, its colony density was increasing with the incubation

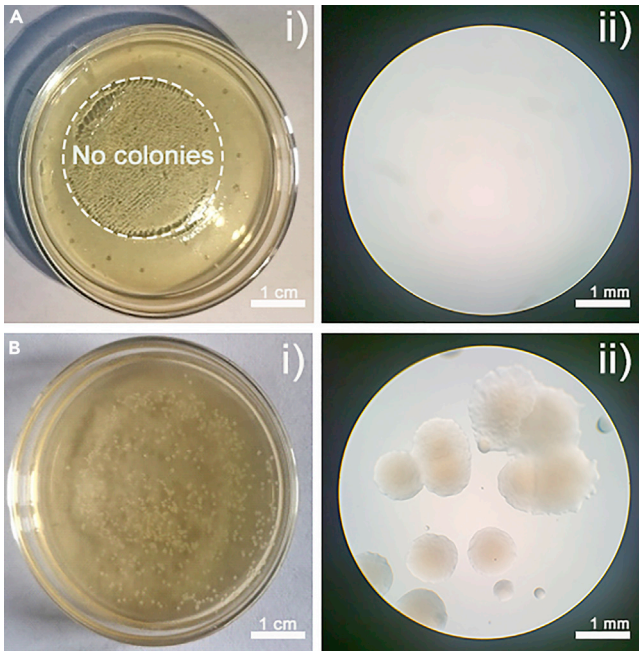

Figure 10. The antibacterial property of Ag/PDA@textile

(A and B) Optical and microscopic images to show the growth status of *E. coli* colony in the agar plate covering with (A) and without (B) Ag/PDA@textile.

time going on (see Figure 10B). These results demonstrated that the Ag/PDA@textile was able to significantly inhibit the growth of *E. coli*, and thus it is hoped to be used in complex conditions.

Conclusions

The Ag/PDA@textile has been developed by chemically depositing Ag particles on the textile surface using polydopamine as the binder layer. The Ag/PDA@textile displays both superhydrophilicity and superoleophobicity in air and underwater and also exhibits water-attracting and oil-resistance when immersed into oil bath. The surface wetting property is retained even after a series of mechanical tests as well as long-term water immersion. Utilizing its opposite surface wetting property between water and oil, Ag/PDA@textile is applied as a separation membrane to separate oil/water mixtures effectively. Water is permeating through the membrane and is collected in the container underneath, while oil is retained above the separation membrane surface. The Ag/PDA@textile also has high repellency to low-polar oils but possesses a strong affinity to oils with high polarity, which allows it to separate immiscible oil/oil mixtures with different polarities efficiently. Owing to the catalytic performance of the Ag particle, organic dyes dissolved in water are decomposed effectively by the Ag/PDA@textile under UV illustration or in the presence of $NaBH_4$. Finally, the Ag/PDA@textile can significantly inhibit the growth of *E. coli*, because of its antibacterial property. Considering the simple fabrication and versatility of the Ag/PDA@textile, this study would help meet the growing needs for liquid waste treatment in the fields of water purification, oily sewage treatment, clean-up of oil spills, and others.

Limitations of the study

Considering the simple fabrication and versatility of the Ag/PDA@textile (see Table S1), this study would help meet the growing needs for liquid waste treatment in the fields of water purification, oily sewage treatment, clean-up of oil spills, and others

STAR★METHODS

Detailed methods are provided in the online version of this paper and include the following:

- KEY RESOURCE TABLE

SUPPLEMENTAL INFORMATION

Supplemental information can be found online at https://doi.org/10.1016/j.isci.2022.104213.

ACKNOWLEDGMENTS

The authors were grateful for the financial support from the Natural Science Foundation of Shandong Province (ZR2019MEM044).

AUTHOR CONTRIBUTIONS

Gan Miao, Fangchao Li, and Zhongshuai Gao performed the experiments and data curation analysis. Ting Xu performed the experiments, methodology, and discussion. Gan Miao designed the experiments, performed the experiments, formal analysis, methodology, investigation, and writing. Xiaotao Zhu designed the project, designed the experiments, modified the original draft, and supervised.

DECLARATION OF INTERESTS

The authors declare no competing interests.

Received: December 27, 2021
Revised: March 16, 2022
Accepted: April 1, 2022
Published: May 20, 2022

SUPPORTING CITATIONS

The following references appear in the supplemental information (Fowkes, 1964; Owens and Wendt, 1969; Rabinovich and Derjaguin, 1988).

REFERENCES

Ai, L., and Zeng, Y. (2013). Hierarchical porous NiO architectures as highly recyclable adsorbents for effective removal of organic dye from aqueous solution. Chem. Eng. J. *215–216*, 269–278.

Akram Shaikh, W., Chakraborty, S., and Islam, R. (2018). UV-assisted photo-catalytic degradation of anionic dye (Congo red) using biosynthesized silver nanoparticles: a green catalysis. Desalin. Water Treat. *130*, 132–142.

Berg, J.M., Eriksson, L.G.T., Claesson, P.M., and Borve, K.G.N. (1994). Three-component Langmuir-blodgett films with a controllable degree of polarity. Langmuir *10*, 1225–1234.

Chen, T., Liu, Z., Zhang, K., Su, B., Hu, Z., Wan, H., Chen, Y., Fu, X., and Gao, Z. (2021). Mussel-inspired Ag NPs immobilized on melamine sponge for reduction of 4-nitrophenol, antibacterial applications and its superhydrophobic derivative for oil–water separation. ACS Appl. Mater. Inter. *13*, 50539–50551.

Chen, X., Zheng, Z.F., Ke, X.B., Jaatinen, E., Xie, T.F., Wang, D.J., Guo, C., Zhao, J.C., and Zhu, H.Y. (2010). Supported silver nanoparticles as photocatalysts under ultraviolet and visible light irradiation. Green. Chem. *12*, 414–419.

Dai, J., Wang, L., Wang, Y., Tian, S., Tian, X., Xie, A., Zhang, R., Yan, Y., and Pan, J. (2020). Robust nacrelike graphene oxide-calcium carbonate hybrid mesh with underwater superoleophobic property for highly efficient oil/water separation. ACS Appl. Mater. Inter. *12*, 4482–4493.

Drelich, J., and Chibowski, E. (2010). Superhydrophilic and superwetting surfaces: definition and mechanisms of control. Langmuir *26*, 18621–18623.

Fowkes, F.M. (1964). Attractive forces at interfaces. J. Ind. Eng. Chem. *56*, 40–52.

Fowkes, F.M., Huang, Y.C., Shah, B.A., Kulp, M.J., and Lloyd, T.B. (1988). Surface and colloid chemical studies of gamma iron oxides for magnetic memory media. Colloids Surf. *29*, 243–261.

Garcia, M.A. (2011). Surface plasmons in metallic nanoparticles: fundamentals and applications. J. Phys. D Appl. Phys. *44*, 283001.

Ge, J., Zhao, H.Y., Zhu, H.W., Huang, J., Shi, L.A., and Yu, S.H. (2016). Advanced sorbents for oil-spill cleanup: recent advances and future perspectives. Adv. Mater. *28*, 10459–10490.

Guan, F., Song, Z., Xin, F., Wang, H., Yu, D., Li, G., and Liu, W. (2020). Preparation of hydrophobic transparent paper via using polydimethylsiloxane as transparent agent. J. Bioresour. Bioprod. *5*, 37–43.

Gupta, R.K., Dunderdale, G.J., England, M.W., and Hozumi, A. (2017). Oil/water separation techniques: a review of recent progresses and future directions. J. Mater. Chem. A. *5*, 16025–16058.

Han, X., and Gong, X. (2021). In situ, one-pot method to prepare robust superamphiphobic cotton fabrics for high buoyancy and good antifouling. ACS Appl. Mater. Inter. *13*, 31298–31309.

Horváth, I.T., and Rábai, J. (1994). Facile catalyst separation without water: fluorous biphase hydroformylation of olefins. Science *266*, 72–75.

Islam, M.R., Ferdous, M., Sujan, M.I., Mao, X., Zeng, H., and Azam, M.S. (2020). Recyclable Ag-decorated highly carbonaceous magnetic nanocomposites for the removal of organic pollutants. J. Colloid Interf. Sci. *562*, 52–62.

Jung, Y.C., and Bhushan, B. (2009). Wetting behavior of water and oil droplets in three-phase interfaces for hydrophobicity/philicity and oleophobicity/philicity. Langmuir *25*, 14165–14173.

Kang, S., Liao, C., and Po, S.-T. (2000). Decolorization of textile wastewater by photo-fenton oxidation technology. Chemosphere *41*, 1287–1294.

Karthik, R., Govindasamy, M., Chen, S.M., Cheng, Y.H., Muthukrishnan, P., Padmavathy, S., and Elangovan, A. (2017). Biosynthesis of silver nanoparticles by using Camellia japonica leaf extract for the electrocatalytic reduction of nitrobenzene and photocatalytic degradation of Eosin-Y. J. Photochem. Photobiol. B *170*, 164–172.

Khare, P., Singh, A., Verma, S., Bhati, A., Sonker, A.K., Tripathi, K.M., and Sonkar, S.K. (2018). Sunlight-induced selective photocatalytic degradation of methylene blue in bacterial culture by pollutant soot derived nontoxic graphene nanosheets. ACS Sustain. Chem. Eng. *6*, 579–589.

Larmour, I.A., Bell, S.E.J., and Saunders, G.C. (2007). Remarkably simple fabrication of superhydrophobic surfaces using electroless galvanic deposition. Angew. Chem. Int. Ed. *46*, 1710–1712.

Lee, Y.H., Kim, A.L., Park, Y.G., Hwang, E.K., Baek, Y.M., Cho, S., and Kim, H.D. (2018). Colorimetric assay and deodorizing/antibacterial performance of natural fabrics dyed with immature pine cone extract. Text. Res. J. *88*, 731–743.

Liu, M., Li, J., Hou, Y., and Guo, Z. (2017). Inorganic adhesives for robust superwetting surfaces. ACS Nano *11*, 1113–1119.

Lu, J., Li, F., Miao, G., Miao, X., Ren, G., Wang, B., Song, Y., Li, X., and Zhu, X. (2021). Superhydrophilic/superoleophobic shell powder coating as a versatile platform for both oil/water and oil/oil separation. J. Membr. Sci. *637*, 119624.

Lu, J.W., Zhu, X.T., Miao, X., Song, Y.M., Liu, L., Ren, G.N., and Li, X.M. (2020). Photocatalytically active superhydrophilic/superoleophobic coating. ACS Omega *5*, 11448–11454.

Ma, Q.L., Cheng, H.F., Fane, A.G., Wang, R., and Zhang, H. (2016). Recent development of advanced materials with special wettability for selective oil/water separation. Small *12*, 2186–2202.

Mai, V.C., Das, P., Ronn, G., Zhou, J.J., Lim, T.T., and Duan, H.W. (2020). Hierarchical graphene/metal-organic framework composites with tailored wettability for separation of immiscible liquids. ACS Appl. Mater. Inter. *12*, 35563–35571.

Matsubayashi, T., Tenjimbayashi, M., Komine, M., Manabe, K., and Shiratori, S. (2017). Bioinspired hydrogel-coated mesh with superhydrophilicity and underwater superoleophobicity for efficient and ultrafast oil/water separation in harsh environments. Ind. Eng. Chem. Res. *56*, 7080–7085.

McFarland, M. (1992). Investigations of the environmental acceptability of fluorocarbon alternatives to chlorofluorocarbons. Proc. Natl. Acad. Sci. U S A *89*, 807–811.

Niyonshuti, I.I., Krishnamurthi, V.R., Okyere, D., Song, L., Benamara, M., Tong, X., Wang, Y., and Chen, J. (2020). Polydopamine surface coating synergizes the antimicrobial activity of silver nanoparticles. ACS Appl. Mater. Inter. *12*, 40067–40077.

Nyiredy, S., Botz, L., and Sticher, O. (1990). Forced-flow multi-phase liquid extraction, a separation method based on relative and absolute counter-current distribution: I. Description of the method and basic possibilities. J. Chromatogr. A. *523*, 43–52.

Owens, D.K., and Wendt, R.C. (1969). Estimation of the surface free energy of polymers. J. Appl. Polym. Sci. *13*, 1741–1747.

Peng, Y.B., and Guo, Z.G. (2016). Recent advances in biomimetic thin membranes applied in emulsified oil/water separation. J. Mater. Chem. A. *4*, 15749–15770.

Qamar, M.A., Shahid, S., Javed, M., Sher, M., Iqbal, S., Bahadur, A., and Li, D.X. (2021). Fabricated novel g-C_3N_4/Mn doped ZnO nanocomposite as highly active photocatalyst for the disinfection of pathogens and degradation of the organic pollutants from wastewater under sunlight radiations. Colloids Surf. A. Physicochem. Eng. Asp. *611*, 125863.

Qiu, L., Sun, Y.H., and Guo, Z.G. (2020). Designing novel superwetting surfaces for high-efficiency oil-water separation: design principles, opportunities, trends and challenges. J. Mater. Chem. A. *8*, 16831–16853.

Rabinovich, Y.I., and Derjaguin, B.V. (1988). Interaction ofhydrophobized filaments in aqueous electrolyte solutions. Colloids Surf. *30*, 243–251.

Sahoo, C., Gupta, A.K., and Pal, A. (2005). Photocatalytic degradation of Methyl Red dye in aqueous solutions under UV irradiation using Ag^+ doped TiO_2. Desalination *181*, 91–100.

Sarcletti, M., Vivod, D., Luchs, T., Rejek, T., Portilla, L., Müller, L., Dietrich, H., Hirsch, A., Zahn, D., and Halik, M. (2019). Superoleophilic magnetic Iron oxide nanoparticles for effective hydrocarbon removal from water. Adv. Funct. Mater. *29*, 1805742.

Sarina, S., Waclawik, E.R., and Zhu, H.Y. (2013). Photocatalysis on supported gold and silver nanoparticles under ultraviolet and visible light irradiation. Green. Chem. *15*, 1814–1833.

Schrope, M. (2011). Oil spill: deep wounds. Nature *472*, 152–154.

Sharif, H.M.A., Mahmood, A., Cheng, H.Y., Djellabi, R., Ali, J., Jiang, W.L., Wang, S.-S., Haider, M.R., Mahmood, N., and Wang, A. (2019). Fe_3O_4 nanoparticles coated with EDTA and Ag nanoparticles for the catalytic reduction of organic dyes from wastewater. ACS Appl. Nano Mater. *2*, 5310–5319.

Singh, M.K., and Mehata, M.S. (2019). Phase-dependent optical and photocatalytic performance of synthesized titanium dioxide (TiO_2) nanoparticles. Optik *193*, 163011.

Tang, H., Fu, Y.H., Yang, C., Zhu, D.N., and Yang, J. (2016). A UV-driven superhydrophilic/superoleophobic polyelectrolyte multilayer film on fabric and its application in oil/water separation. RSC Adv. *6*, 91301–91307.

Tie, L., Li, J., Liu, M.M., Guo, Z.G., Liang, Y.M., and Liu, W.M. (2018). Organic media superwettability: on-demand liquid separation by controlling surface chemistry. ACS Appl. Mater. Inter. *10*, 37634–37642.

Tiwari, J.N., Mahesh, K., Le, N.H., Kemp, K.C., Timilsina, R., Tiwari, R.N., and Kim, K.S. (2013). Reduced graphene oxide-based hydrogels for the efficient capture of dye pollutants from aqueous solutions. Carbon *56*, 173–182.

Vogler, E.A. (1998). Structure and reactivity of water at biomaterial surfaces. Adv. Colloid Interf. Sci. *74*, 69–117.

Wang, B., Liang, W.X., Guo, Z.G., and Liu, W.M. (2015a). Biomimetic super-lyophobic and super-lyophilic materials applied for oil/water separation: a new strategy beyond nature. Chem. Soc. Rev. *44*, 336–361.

Wang, L., He, H., Yu, Y.B., Sun, L., Liu, S.J., Zhang, C.B., and He, L. (2014). Morphology-dependent bactericidal activities of Ag/CeO_2 catalysts against Escherichia coli. J. Inorg. Biochem. *135*, 45–53.

Wang, L., Zhao, Y., Tian, Y., and Jiang, L. (2015b). A general strategy for the separation of immiscible organic liquids by manipulating the surface tensions of nanofibrous membranes. Angew. Chem. Int. Ed. *54*, 14732–14737.

Wang, Y., Di, J.C., Wang, L., Li, X., Wang, N., Wang, B.X., Tian, Y., Jiang, L., and Yu, J.H. (2017). Infused-liquid-switchable porous nanofibrous membranes for multiphase liquid separation. Nat. Commun. *8*, 575.

Wei, D.W., Wei, H., Gauthier, A.C., Song, J., Jin, Y., and Xiao, H. (2020). Superhydrophobic

modification of cellulose and cotton textiles: methodologies and applications. J. Bioresour. Bioprod. *5*, 1–15.

Wenzel, R.N. (1936). Resistance of solid surfaces to wetting by water. J. Ind. Eng. Chem. *28*, 988–994.

Wu, Z., Zhang, Y., Tao, T., Zhang, L., and Fong, H. (2010). Silver nanoparticles on amidoxime fibers for photo-catalytic degradation of organic dyes in waste water. Appl. Surf. Sci. *257*, 1092–1097.

Xie, Y.J., Yan, B., Xu, H.L., Chen, J., Liu, Q.X., Deng, Y.H., and Zeng, H.B. (2014). Highly regenerable mussel-inspired Fe_3O_4@Polydopamine-Ag core-shell microspheres as catalyst and adsorbent for methylene blue removal. ACS Appl. Mater. Inter. *6*, 8845–8852.

Xu, Q.B., Xie, L.J., Diao, H.L.N., Li, F., Zhang, Y.Y., Fu, F.Y., and Liu, X.D. (2017). Antibacterial cotton fabric with enhanced durability prepared using silver nanoparticles and carboxymethyl chitosan. Carbohydr. Polym. *177*, 187–193.

Xu, Z.G., Zhao, Y., Wang, H.X., Wang, X.G., and Lin, T. (2015). A superamphiphobic coating with an ammonia-triggered transition to superhydrophilic and superoleophobic for oil-water separation. Angew. Chem. Int. Ed. *54*, 4527–4530.

Yan, L., Li, H., Li, W., Zha, F., and Lei, Z. (2015). Underwater superoleophobic palygorskite coated meshes for efficient oil/water separation. J. Mater. Chem. A. *3*, 14696–14702.

Yan, L., Li, P., Zhou, W., Wang, Z., Fan, X., Chen, M., Fang, Y., and Liu, H. (2019). Shrimp shell-inspired antifouling chitin nanofibrous membrane for efficient oil/water emulsion separation with in situ removal of heavy metal ions. ACS Sustain. Chem. Eng. *7*, 2064–2072.

Yang, J., Zhang, Z.Z., Xu, X.H., Zhu, X.T., Men, X.H., and Zhou, X.Y. (2012). Superhydrophilic-superoleophobic coatings. J. Mater. Chem. *22*, 2834–2837.

Yong, J.L., Chen, F., Yang, Q., Huo, J.L., and Hou, X. (2017). Superoleophobic surfaces. Chem. Soc. Rev. *46*, 4168–4217.

Yu, H., Wu, M., Duan, G., and Gong, X. (2022). One-step fabrication of eco-friendly superhydrophobic fabrics for high-efficiency oil/water separation and oil spill cleanup. Nanoscale *14*, 1296–1309.

Yu, L., Han, M., and He, F. (2017). A review of treating oily wastewater. Arab. J. Chem. *10*, S1913–S1922.

Zhang, D., Wang, G., Zhi, S., Xu, K., Zhu, L., Li, W., Zeng, Z., and Xue, Q. (2018). Superhydrophilicity and underwater superoleophobicity TiO_2/Al_2O_3 composite membrane with ultra low oil adhesion for highly efficient oil-in-water emulsions separation. Appl. Surf. Sci. *458*, 157–165.

Zhang, J.C., Zhang, F., Song, J., Liu, L.F., Si, Y., Yu, J.Y., and Ding, B. (2019). Electrospun flexible nanofibrous membranes for oil/water separation. J. Mater. Chem. A. *7*, 20075–20102.

Zhang, W., Wang, D., Sun, Z., Song, J., and Deng, X. (2021). Robust superhydrophobicity: mechanisms and strategies. Chem. Soc. Rev. *50*, 4031–4061.

Zhang, W.B., Zhu, Y.Z., Liu, X., Wang, D., Li, J.Y., Jiang, L., and Jin, J. (2014). Salt-induced fabrication of superhydrophilic and underwater superoleophobic PAA-g-PVDF membranes for effective separation of oil-in-water emulsions. Angew. Chem. Int. Ed. *53*, 856–860.

Zheng, Y., and Wang, A. (2012). Ag nanoparticle-entrapped hydrogel as promising material for catalytic reduction of organic dyes. J. Mater. Chem. *22*, 16552–16559.

Zhu, X., Zhang, Z., Yang, J., Xu, X., Men, X., and Zhou, X. (2012). Facile fabrication of a superhydrophobic fabric with mechanical stability and easy-repairability. J. Colloid Interf. Sci. *380*, 182–186.

STAR★METHODS

KEY RESOURCE TABLE

REAGENT or RESOURCE	SOURCE	IDENTIFIER
Chemicals, Peptides, and Recombinant Proteins		
Dopamine hydrochloride	Sigma-Aldrich	CSA:62-31-7
Tris(hydroxymethyl)aminomethane	Aladdin	CSA:77-86-1
Ammonia solution	Sinopharm Chemical Reagent	CSA:1336-21-6
Silver nitrate	Sinopharm Chemical Reagent	CSA:7761-88-8
Methylene blue	Sinopharm Chemical Reagent	CSA:7220-79-3
Glucose	Aladdin	CSA:604-68-2
Sodium borohydride	Sinopharm Chemical Reagent	CSA:16940-66-2
perfluorooctanoic acid	Sigma-Aldrich	CSA:335-67-1
Acetone	Sinopharm Chemical Reagent	CSA:67-64-1
Alcohol	Sinopharm Chemical Reagent	CSA:64-17-5
Other		
Textiles	Local stores	

RESOURCE AVAILABILITY

Lead contact

Further information and requests for resources and reagents should be directed to and will be fulfilled by the lead contact, Xiaotao Zhu (xiaotao.zhu@ytu.edu.cn).

Materials availability

This study did not generate nor use any new or unique reagents.

Data and code availability

- This study did not generate any unique code or data sets.
- All data supporting the finding of this study are available within the paper and its Supplemental information files.
- Any additional information required to reanalyze the data reported in this paper is available from the Lead contact upon request.
- All software's used in this study are commercially available.

METHOD DETAILS

Materials and chemicals

Tris(hydroxymethyl) aminomethane hydrochloride (Tris, ≥98.0%) was obtained from Aladdin Chemicals (Shanghai, China). Dopamine hydrochloride (DA, 98%) and perfluorooctanoic acid (denoted as PFOA) was acquired from Sigma-Aldrich. Ammonia solution (25–27 wt %), silver nitrate, methylene blue (MB), and glucose were provided by Sinopharm Chemical Reagent Co., Ltd., China. Sodium borohydride ($NaBH_4$) was obtained from Fisher Scientific. Sodium perfluorooctanoate (denoted PFOA-Na) with a concentration of 1.0 M was fabricated by the reaction of NaOH and PFOA in ethanol. The commercially available textiles made of cellulose were bought from local stores and ultrasonically cleaned with acetone, alcohol, and deionized water for 20 min in sequence before use. All reagents related to *E. coli* (*E. coli*) cultures were purchased TaKaRa (Dalian, China).

Preparation of PDA@textile

The polydopamine (PDA) deposited textile (PDA@textile) was created by coating the textile with a PDA layer. Briefly, 120 mg of Tris was dissolved in 100 mL of deionized water to make the solution slightly alkaline

(pH = 8.5). Then, 50 mg of DA was dispersed in the solution. The textile was immersed in the above solution under stirring. After 24 h reaction, the PDA@textile was obtained.

Preparation of Ag/PDA@textile

2 mL ammonia solution was dropped into 12 mL silver nitrate solution (0.1 g/mL) to create a transparent solution, and then the PDA@textile immerse in this solution for 15 min. Subsequently, the textile was transferred into a 50 mL glucose solution (50 g/L) for about 3 h, which allowed an Ag layer to be deposited on the PDA/textile surface. Finally, the Ag deposited PDA@textile (denoted as Ag/PDA@textile) was immersed into 1.0 M PFOA-Na ethanol solution for 5 min and washed with deionized water to achieve a slippery oil-repellent state.

Characterizations

Contact angle (CA) and sliding angle (SA) were measured at environmental temperature using a Krüss DSA 100 (Krüss Company, Ltd., Germany) instrument. Scanning electron microscopy images were carried out by JSM-6701F field-emission scanning electron microscopy (FESEM, JEOL, Japan) equipped with Energy-dispersive X-ray spectroscopy (EDS). The chemical composition of the original and superoleophobic textile was detected using the attenuated total reflectance Fourier transform infrared spectrometer (ATR-FTIR, Nicolet 6700, Thermoelectric Scientific Instruments Corp, USA). The elemental composition of the textile was systematically characterized using X-ray photoelectron spectroscopy (XPS, AXIS SUPRA). The optical images were obtained by a digital camera (Nikon). The UV-visible absorption spectroscopy data of MB were determined by a HITACHI U-3010 UV-vis spectrophotometer. Thermal images were collected, using an IR Thermal Camera (FLIR Ts-650). The colony morphology was viewed by a microscope (Eclipse 80i, Nikon, Japan). The optical images were acquired by the digital camera (Nikon).

Separation efficiency analysis

Place the Ag/PDA@textile on a membrane holder between two glass tubes and pour the mixture of oil/oil and oil/water on top. The separation efficiency of oil/water and oil/oil is obtained by the formula below:

$$\text{Separation efficiency (\%)} = M1/M2 \times 100\%$$

In which M_1 and M_2 represent the weight of the liquid collected below following the separation and the original weight of the liquid before the separation, respectively.

Emulsion separation analysis

Tween 80-stabilized toluene in water (O/W) emulsions were prepared (5 wt %), Ag/PDA@textile was used as a filter module to separate O/W emulsions. Herein, we developed optical microscope analysis to study the distributed droplets in the O/W feed emulsions and filtrates.

Conductivity testing

Ag/PDA@textile (size: 40 ×10 × 1 mm) is used as part of the external circuit in different states, and the brightness difference of small light bulbs is used to characterize the conductivity of Ag/PDA@textile.

Removal of organic dyes from water

The Ag/PDA@textile (size: 10 ×10 × 1 mm) was used as a catalyst for decomposition MB under UV irradiation at 254 nm, and it was put into 8 mL of MB aqueous solution (20 mg/L) at room temperature. The MB decomposition can be accelerated by our Ag/PDA@textile by adding 0.5 mL of $NaBH_4$ aqueous solution (0.2 mol/L) into the MB aqueous solution. The content of MB in the solution was monitored through the measurement of the change in absorbance at 665 nm using a UV-Vis spectrophotometer.

Antimicrobial evaluation

The antimicrobial test is performed by typical pathogens, *E. coli* (Gram-negative). Ag/PDA@textile was cut into a 3 cm diameter circle. All glassware and membranes for the solution are autoclaved. Briefly, *E. coli* was pre-cultured and diluted in nutritional broth to obtain the needed test inoculum. Then, evenly distribute 0.3 mL of the test inoculum on an agar plate and place the Ag/PDA@textile sample. Petri disshes are cultured at 37°C for 24 h. The growth state of the colony characterizes the antibacterial effect of Ag/PDA/textile.